Extracellular NAD$^+$ shapes the Foxp3$^+$ regulatory T cell compartment through the ART2–P2X7 pathway

Sandra Hubert,[1,2] Björn Rissiek,[4] Katjana Klages,[5] Jochen Huehn,[5] Tim Sparwasser,[6] Friedrich Haag,[4] Friedrich Koch-Nolte,[4] Olivier Boyer,[1,2,3] Michel Seman,[1,7] and Sahil Adriouch[1,2]

[1]Institut National de la Santé et de la Recherche Medicale, U905, [2]University of Rouen, and [3]Department of Immunology, University Hospital of Rouen, 76183 Rouen, France
[4]Institute of Immunology, University Medical Center Hamburg-Eppendorf, 20246 Hamburg, Germany
[5]Experimental Immunology, Helmholtz Centre for Infection Research, 38124 Braunschweig, Germany
[6]Institute of Infection Immunology, Centre for Experimental and Clinical Infection Research, Twincore, 30625 Hannover, Germany
[7]University Denis Diderot - Paris 7, 75000 Paris, France

CD4$^+$CD25$^+$FoxP3$^+$ regulatory T cells (T reg cells) play a major role in the control of immune responses but the factors controlling their homeostasis and function remain poorly characterized. Nicotinamide adenine dinucleotide (NAD$^+$) released during cell damage or inflammation results in ART2.2–mediated ADP-ribosylation of the cytolytic P2X7 receptor on T cells. We show that T reg cells express the ART2.2 enzyme and high levels of P2X7 and that T reg cells can be depleted by intravenous injection of NAD$^+$. Moreover, lower T reg cell numbers are found in mice deficient for the NAD-hydrolase CD38 than in wild-type, P2X7-deficient, or ART2-deficient mice, indicating a role for extracellular NAD$^+$ in T reg cell homeostasis. Even routine cell preparation leads to release of NAD$^+$ in sufficient quantities to profoundly affect T reg cell viability, phenotype, and function. We demonstrate that T reg cells can be protected from the deleterious effects of NAD$^+$ by an inhibitory ART2.2-specific single domain antibody. Furthermore, selective depletion of T reg cells by systemic administration of NAD$^+$ can be used to promote an antitumor response in several mouse tumor models. Collectively, our data demonstrate that NAD$^+$ influences survival, phenotype, and function of T reg cells and provide proof of principle that acting on the ART2–P2X7 pathway represents a new strategy to manipulate T reg cells in vivo.

CORRESPONDENCE
Michel Seman:
michel.seman@univ-rouen.fr
OR
Sahil Adriouch: sahil.adriouch@univ-rouen.fr

Abbreviations used: ART, ADP-ribosyltransferase; GzB, granzyme B; NAD$^+$, nicotinamide adenine dinucleotide; NICD, NAD-induced cell death; PI, propidium iodide; PS, phosphatidylserine; sdAb, single domain antibody; T conv cell, conventional T cell; TIL, tumor-infiltrating lymphocyte; T reg cell, regulatory T cell.

Immunological self-tolerance is critical for the prevention of autoimmunity and maintenance of immune homeostasis. CD4$^+$CD25$^+$ regulatory T cells (T reg cells) play a major role in this process and represent a T cell subset of thymic origin that is dependent on the expression of the forkhead family transcription factor Foxp3 (Fontenot et al., 2003; Hori et al., 2003). T reg cells have been shown to down-regulate many types of immune responses, including potentially harmful effector immune reactions (Sakaguchi, 2005). However, the pathways that lead to the induction of Foxp3 expression and control T reg cell development and homeostasis remain largely unknown. Foxp3 deficiency leads to the *scurfy* phenotype in mice and to the life-threatening IPEX (immunodysregulation polyendocrinopathy enteropathy X-linked) syndrome in humans, a disease characterized by extensive lymphoproliferation and multiple autoimmune disorders (Ochs et al., 2005). In contrast, Foxp3 overexpression in transgenic mice causes lymphopenia and immunodeficiency (Khattri et al., 2001). Efficient control of the T reg cell population size and function is thus necessary to ensure a balance between self-tolerance and immune responsiveness.

Extracellular nucleotides may play a central role in this process. Notably, ATP and

S. Hubert and B. Rissiek contributed equally to this paper.

The Rockefeller University Press $30.00
J. Exp. Med. Vol. 207 No. 12 2561-2568
www.jem.org/cgi/doi/10.1084/jem.20091154

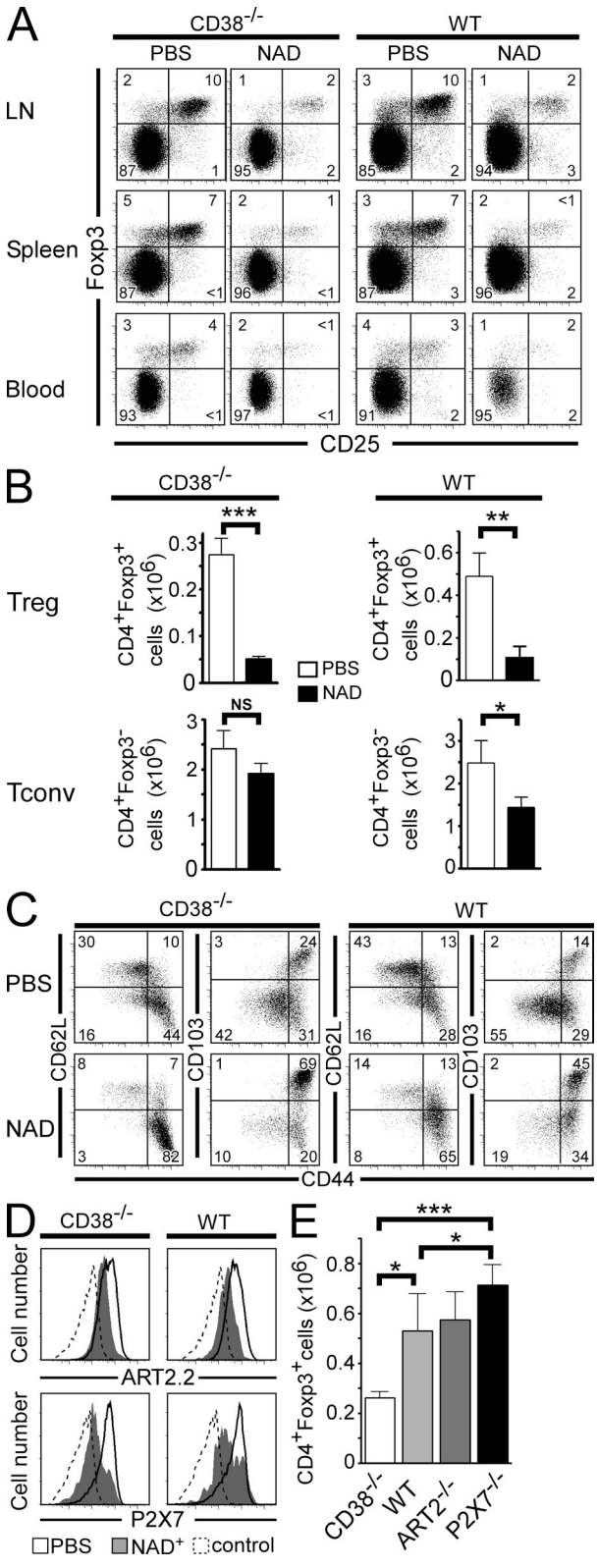

Figure 1. T reg cells are sensitive to NICD in vivo. CD38$^{-/-}$ and WT mice were injected i.v. with either 10 or 60 mg NAD$^+$, respectively, or with PBS and analyzed 24 h later. (A) LN, spleen, and blood cells were stained for CD4, CD25, and Foxp3 and analyzed by flow cytometry. Representative CD25/Foxp3 immunophenotyping data of the CD4$^+$-gated population are shown. Numbers indicate percentage of cells in each quadrant. (B) Histograms represent absolute mean numbers (pool of six LNs) of CD4$^+$Foxp3$^+$ or CD4$^+$Foxp3$^-$ cells from CD38$^{-/-}$ or WT mice that had been injected with NAD$^+$. (C) Flow cytometry analyses of the expression of CD44, CD62L, and CD103 on the surface of CD4$^+$Foxp3$^+$ gated T reg cells 24 h after systemic administration of NAD$^+$. Numbers indicate percentage of cells in each quadrant. (D) Flow cytometry analyses of the expression of ART2.2 and P2X7 on the surface of CD4$^+$Foxp3$^+$ gated T reg cells 24 h after systemic administration of NAD$^+$ (shaded histogram) or PBS (open histogram). Negative staining controls are depicted by a dashed line. (E) Histograms represent absolute mean numbers of CD4$^+$Foxp3$^+$ T cells enumerated from six pooled LNs harvested from the indicated mice. Data are representative of at least three independent experiments, each one performed with a minimum of five mice per group. Error bars represent SEM. *, $P < 0.05$; **, $P < 0.01$; ***, $P < 0.001$.

nicotinamide adenine dinucleotide (NAD$^+$) released by cell lysis or nonlytic mechanisms (Bruzzone et al., 2001; Contreras et al., 2002) can activate the P2X7 receptor and induce T cell death (Seman et al., 2003; Scheuplein et al., 2009). P2X7 is an ATP-gated ion channel expressed on many cells of the immune system (Di Virgilio et al., 2001). On T cells, we previously showed that P2X7 activation induces rapid shedding of CD62L, externalization of phosphatidylserine (PS) on the cell surface, and, ultimately, cell death (Seman et al., 2003; Scheuplein et al., 2009). On macrophages, it also causes membrane blebbing and caspase-dependent release of proinflammatory cytokines such as IL-1β and IL-18 (Di Virgilio, 2007). Remarkably, however, although relatively high ATP concentrations (0.2–1 mM) are required for P2X7 activation, we have shown that micromolar concentrations of NAD$^+$ are sufficient to activate P2X7 on mouse T lymphocytes (Seman et al., 2003). This results from ADP ribosylation of P2X7 on arginine 125 mediated by the mono–ADP-ribosyltransferase (ART) ART2.2 (Adriouch et al., 2008), which catalyzes the covalent transfer of the ADP-ribose group from NAD$^+$ onto arginine residues of membrane target proteins (Seman et al., 2003). Consequently, NAD$^+$ released during inflammation participates in the regulation of T cell homeostasis in vivo through an ART2.2-dependent P2X7-mediated mechanism (Adriouch et al., 2007), a process which is now referred to as NAD-induced cell death (NICD; Seman et al., 2003). NICD is controlled in part by the NAD-glycohydrolase CD38, which limits substrate availability for ART2.2 by hydrolyzing extracellular NAD$^+$ (Krebs et al., 2005).

It has recently been shown that mouse Foxp3$^+$ T reg cells are susceptible to cell death induced by exogenous nucleotides (Aswad et al., 2005), but little is known about the role of NICD in vivo and its consequences on T reg cell homeostasis. Hence, we investigated how NAD$^+$ could regulate the T reg cell compartment by analyzing T reg cell number, phenotype, and function in mice deficient for P2X7, ART2, or CD38. We demonstrate that endogenous NAD$^+$ indeed controls the pool of Foxp3$^+$ T cells by an ART2/P2X7-dependent process and that NAD$^+$ released during preparation of primary

lymphocytes profoundly affects T reg cell phenotype and function. Moreover, we provide proof of principle that it is possible to manipulate T reg cells in vivo via the ART2–P2X7 pathway: an ART2.2-blocking single domain antibody (sdAb) can be used to protect T reg cells from NAD^+-induced cell death, whereas, conversely, NAD^+ can be used to dampen T reg cell function and promote antitumor responses.

RESULTS AND DISCUSSION

Susceptibility of T reg cells to extracellular NAD^+ in vivo

To evaluate the effect of NAD^+ on T reg cells in vivo, we analyzed the compartment of $CD4^+CD25^+Foxp3^+$ T cells after i.v. injection of NAD^+. For this, we used WT and $CD38^{-/-}$ mice that lack the major enzyme responsible for extracellular NAD^+ degradation and in which the bioavailability of NAD^+ is augmented (Partida-Sánchez et al., 2001; Krebs et al., 2005). When analyzed in terms of relative cell frequency and absolute cell number, NAD treatment led to a 75–80% reduction of T reg cell frequency in both WT and $CD38^{-/-}$ mice, although a sixfold higher dose of NAD^+ was required to induce comparable effects in WT mice (Fig. 1, A and B). Analysis of the effect of NAD^+ on $CD4^+Foxp3^-$ conventional T cells (T conv cells) revealed that they were dramatically less sensitive to NAD^+ than their T reg cell counterparts (Fig. 1 B). 1 d after NAD treatment, surviving T reg cells were enriched in cells with a classical activated/memory phenotype, i.e., $CD44^{hi}$ $CD62L^{lo}CD103^+$ (Fig. 1 C), and were also $P2X7^{lo}$ and $ART2.2^{lo}$ (Fig. 1 D), suggesting that activated/memory T reg cells are less sensitive to NICD than naive T reg cells.

The observation that exogenous NAD^+ can modulate the size and the phenotype of the T reg cell pool in vivo suggested that endogenous NAD^+ could participate in T reg cell homeostasis. To explore this hypothesis, we measured the size of the T reg cell population in LNs from unmanipulated $CD38^{-/-}$, $ART2^{-/-}$, and $P2X7^{-/-}$ mice (Fig. 1 E). The reduced capacity of $CD38^{-/-}$ animals to degrade extracellular NAD^+ was associated with significantly lower numbers of T reg cells than in WT mice (Fig. 1 E). In contrast, mice that are insensitive to NICD because of genetic deletion of ART2.2 or P2X7 had higher numbers of T reg cells, which is consistent with the notion that endogenous NAD^+ shapes the T reg cell compartment in vivo.

High expression of P2X7 by T reg cells correlates with a high sensitivity of T reg cells to NICD

To explore the mechanism accounting for the differential susceptibility of T reg cells and T conv cells to NICD, we further investigated their phenotype in terms of ART2.2 and P2X7 expression and sensitivity to cell death induced by NAD^+ ex vivo. Antibody-based staining for intracellular Foxp3 requires cell permeabilization, precluding a distinction between live and apoptotic or dead cells. DEREG mice, which express a DTR-eGFP fusion protein under the control of the *foxp3* promoter, allow more direct analysis of T reg cells (Lahl et al., 2007). We transferred the transgene from DEREG mice to $CD38^{-/-}$, $ART2^{-/-}$, and $P2X7^{-/-}$ animals by backcrossing.

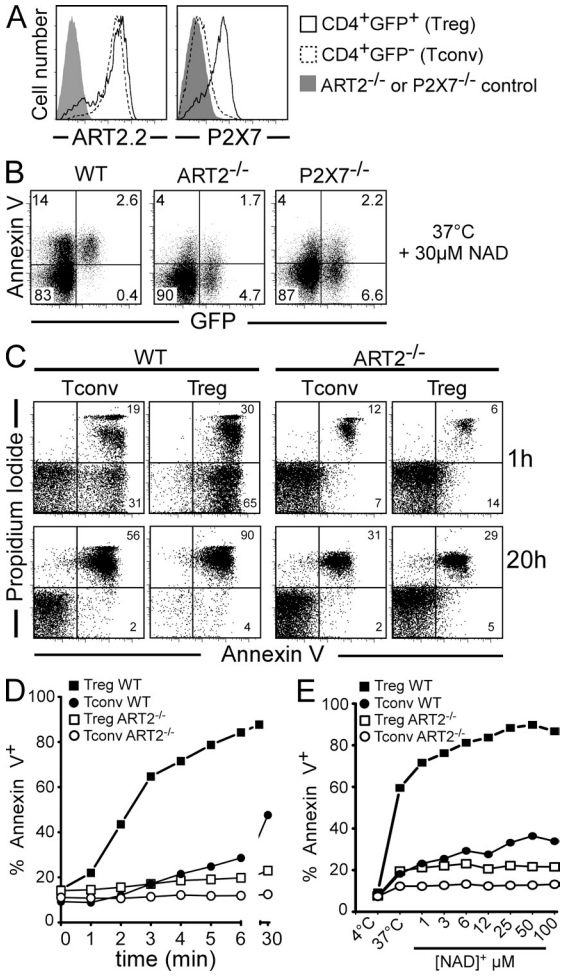

Figure 2. T reg cells express higher levels of cell surface P2X7 and are more sensitive to NICD in vitro than $CD4^+$ T conv cells. (A) Flow cytometry analyses of ART2.2 and P2X7 cell surface expression on $CD4^+$ gated LN cells from DEREG/WT mice (open histograms) or respective DEREG/$ART2^{-/-}$ or DEREG/$P2X7^{-/-}$ mice (shaded histograms). (B) LN cells from DEREG/WT, DEREG/$ART2^{-/-}$, or DEREG/$P2X7^{-/-}$ mice were incubated with 30 µM NAD^+ for 20 min at 37°C before staining with annexin V and flow cytometry analyses. Numbers indicate percentage of cells in each quadrant. (C–E) Splenocytes from DEREG/WT or DEREG/$ART2^{-/-}$ mice were incubated at 37°C with 30 µM NAD^+ for the indicated times (C and D) or with the indicated concentrations of NAD^+ for 15 min (E). Cells were stained with α-CD4 and with annexin V and PI before flow cytometry analyses. T conv cells correspond to $CD4^+GFP^-$ gated population and T reg cells to the $CD4^+GFP^+$ gated population. Data are representative of three independent experiments.

Remarkably, T reg cells showed a higher level of expression of P2X7 than T conv cells (Fig. 2 A). Also, T reg cells displayed ART activity when assayed in vitro (not depicted) and, accordingly, display ART2.2 expression on their surface (Fig. 2 A). Hence, differences in P2X7 expression levels in T conv cells and T reg cells correlate with their differential sensitivity to NICD in vivo (Fig. 1, A and B).

To determine whether the higher sensitivity of T reg cells compared with T conv cells to NAD^+ in vivo is linked to cell-intrinsic differences (e.g., expression level of P2X7) rather

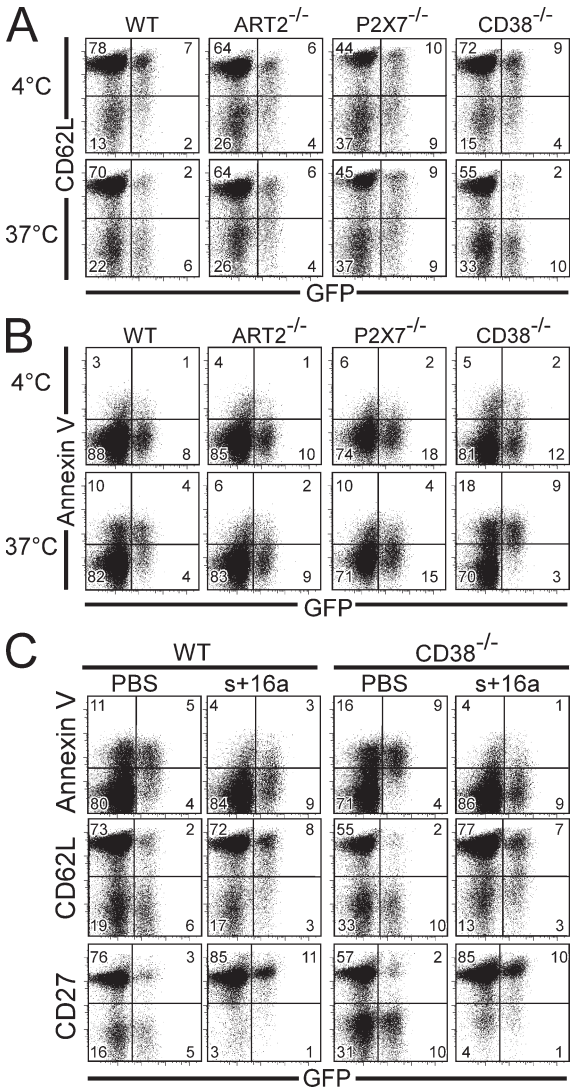

Figure 3. NAD⁺ released during cell preparation induces ART2.2/P2X7-dependent CD62L shedding and PS exposure on T reg cells, which can be prevented by systemic injection of the ART2.2-inhibiting sdAb s+16a. Spleen cells from DEREG/WT, DEREG/ART2$^{-/-}$, DEREG/P2X7$^{-/-}$, and DEREG/CD38$^{-/-}$ mice were collected and kept on ice. Cell suspensions were incubated for 15 min at 4 or 37°C and subsequently stained for CD4, PI, and CD62L (A) or annexin V (B). (C) Splenocytes were obtained from DEREG/WT or DEREG/CD38$^{-/-}$ mice 10 min after systemic injection of PBS or 300 µg of sdAb s+16a. Cells were then incubated for 15 min at 37°C before staining with anti-CD4, PI, and annexin V (top), CD62L (middle), or CD27 (bottom). All FACS data are gated on live (PI$^-$) CD4$^+$ cells. Numbers indicate the percentage of cells in each quadrant. Results are representative of three independent experiments.

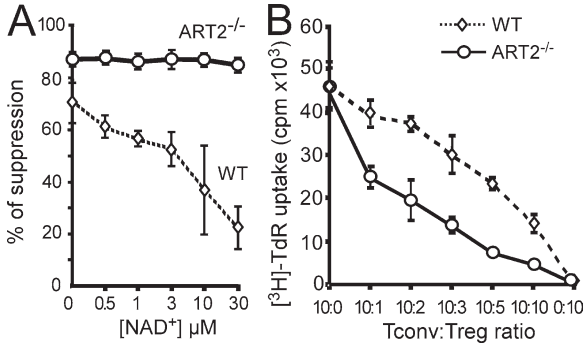

Figure 4. Inhibition of T reg cell suppressive functions in vitro by NAD⁺. (A) CD4$^+$CD25$^+$ T reg cells were isolated from WT or ART2$^{-/-}$ mice and cultured at a 1:1 ratio with CD4$^+$CD25$^-$ T conv cells from an ART2$^{-/-}$ mouse. Cells were stimulated with Con A in the absence or presence of increasing concentrations of exogenously added NAD$^+$. Proliferation was assayed by incorporation of [^{3}H]-TdR on day 3. (B) CD4$^+$CD25$^+$ T reg cells were isolated from WT and ART2$^{-/-}$ mice and cultured with CD4$^+$CD25$^-$ T conv cells from a WT mouse at the indicated ratios. Stimulation of culture and cell proliferation were performed as in A. Data are representative of four independent experiments, each one performed in triplicate. Error bars represent SEM.

than to any other in vivo confounding factor, we conducted a more detailed comparison of the effects of NAD$^+$ on these populations in vitro (Fig. 2, B–E). Incubation of cells with micromolar concentrations of NAD$^+$ induced externalization of PS (Fig. 2, B and C), followed by irreversible uptake of propidium iodide (PI; Fig. 2 C), on the vast majority of T reg cells. NICD of T reg cells was ART2 and P2X7 dependent because it was not observed in cells from ART2$^{-/-}$ or P2X7$^{-/-}$ mice (Fig. 2, B and C). The results of kinetic and dose-response analyses underscore the much higher sensitivity of T reg cells than T conv cells to NICD (Fig. 2, D and E).

NAD⁺ released during preparation of T reg cells causes shedding of CD62L and externalization of PS

Because T reg cells are highly sensitive to NICD, we hypothesized that they might already be profoundly affected by NAD$^+$ released during routine ex vivo isolation. Indeed, we have recently shown that NAD$^+$ released during preparation of primary spleen and LN cells induces ADP ribosylation of P2X7 even at 4°C. When cells are subsequently returned to 37°C, for example, for functional analysis, this results in the activation of P2X7 on a fraction of T cells (Scheuplein et al., 2009). We thus examined whether T reg cells shed CD62L and/or externalize PS on the cell surface as early signs of ART2–P2X7 pathway triggering in vitro. To this end, spleen cells were carefully prepared on ice and were either maintained at 4°C or incubated for 15 min at 37°C. They were subsequently stained with anti-CD62L (Fig. 3 A) or annexin V (Fig. 3 B) for evaluation of P2X7 activation. The results show that most T reg cells from CD38$^{-/-}$ mice spontaneously shed CD62L when incubated at 37°C, as the proportion of CD62L$^+$ cells among the GFP$^+$ T reg cell population dropped from 70 to <20% (Fig. 3 A). A similar effect was observed in cells from WT mice, as >75% T reg cells express CD62L$^+$ when cells were kept at 4°C, whereas only <30% do so upon incubation at 37°C (Fig. 3 A). Importantly, this phenomenon was ART2 and P2X7 dependent because it was not observed in cells from ART2$^{-/-}$ or P2X7$^{-/-}$ mice. Similarly, annexin V staining showed that most T reg cells from both CD38$^{-/-}$ and WT mice undergo spontaneous apoptosis when incubated at 37°C, whereas T reg cells from ART2$^{-/-}$ or P2X7$^{-/-}$ mice

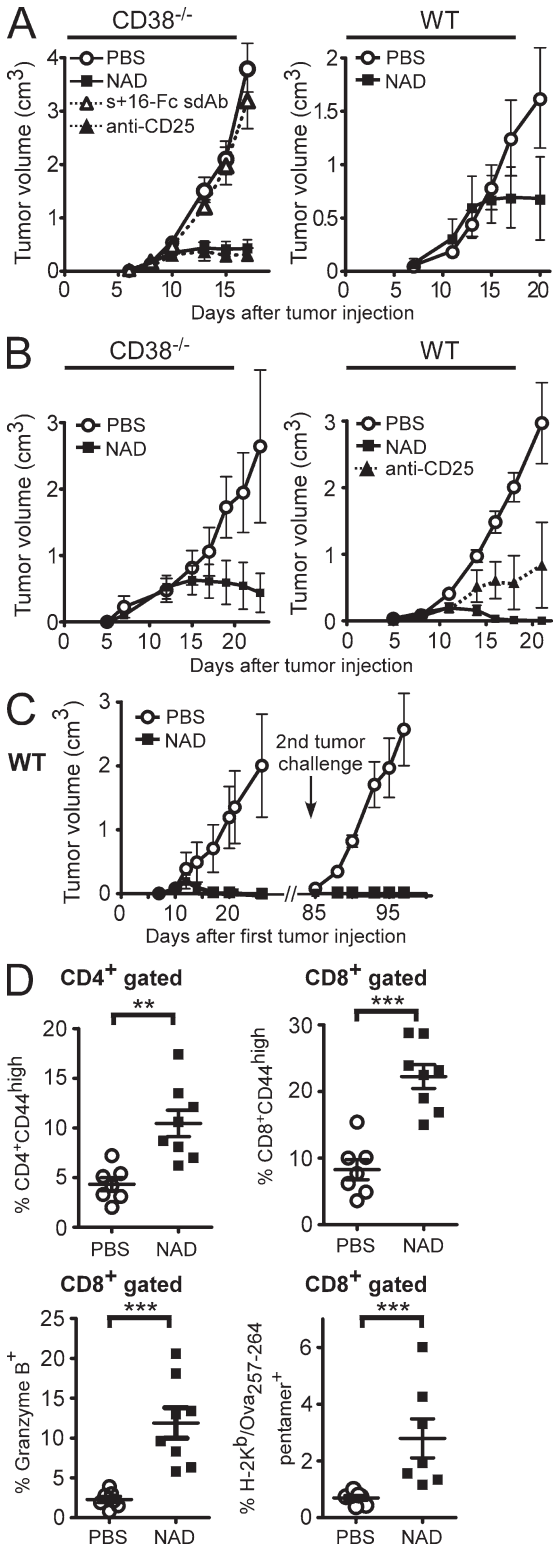

Figure 5. Effect of in vivo administration of NAD+ on the immune response against EL4 and EG7 tumors. (A–D) 2×10^5 EL4 (A) or EG7 (B–D) tumor cells were inoculated s.c. on day 0 into the backs of $CD38^{-/-}$ or WT mice and tumor growth was followed. Groups of mice ($n = 7–8$) received systemic injections of PBS on day −1 (control), anti-CD25 (PC-61) antibody on days −4 and −1, 10 mg ($CD38^{-/-}$) or 60 mg (WT) NAD^+ on day −1, or s+16a-Fc on day −2 followed by NAD injection on day −1. (C) WT mice that had been treated with 60 mg NAD^+ on day −1 and had rejected the primary EG7 tumor received a secondary tumor challenge 2 mo later with a fivefold higher dose of EG7 tumor cells (10^6 cells). Control group of untreated mice were injected in parallel with the same number of EG7 cells. (D) Flow cytometry analyses of lymphocytes from blood samples taken on days 12–14 after inoculation of EG7 tumor cells. Cells were stained for the indicated markers before flow cytometry analyses and gating on $CD4^+$ or $CD8^+$ cells. Data are representative of at least three independent experiments for each tumor model (with $n = 7–8$ mice per group). Statistical Mann-Whitney *U* tests were used and showed significant differences between tumor volumes in all experiments when comparing PBS to NAD-treated animals after day 15. Horizontal lines show the mean. **, $P < 0.01$; ***, $P < 0.001$. Error bars represent SEM.

are resistant (Fig. 3 B). It is of note that incubation of cells at 37°C resulted in a gradual disappearance of T reg cells from the live cell gate used for FACS analyses, a phenomenon which was enhanced upon addition of exogenous NAD^+ or ATP (unpublished data). Collectively, these results show that inadvertent NAD^+ release during preparation of lymphocytes is sufficient to induce NICD on a large fraction of T reg cells. This should be taken into account when interpreting experiments performed using T reg cells isolated ex vivo.

Protection of T reg cells from NICD by a sdAb to ART2.2

We next asked whether T reg cells could be protected from the deleterious effects of NAD^+ by acting on the ART2.2–P2X7 pathway. We recently generated an ART2.2-inhibiting sdAb, designated s+16a, from an immunized llama (Koch-Nolte et al., 2007). One favorable feature of llama sdAbs is a long CDR3 that can extend into and block the active site of a cognate enzyme (De Genst et al., 2006). In vivo, the small (15 kD) sdAbs show rapid penetration into tissues (Cortez-Retamozo et al., 2004). Thus, i.v. injection of sdAb s+16a results in complete blockade of ART2.2 on splenic and LN T cells within 10 min after injection (Koch-Nolte et al., 2007). We tested whether systemic injection of s+16a would protect T reg cells from NICD induced by ex vivo preparation. The results demonstrate that i.v. injection of s+16a 10 min before euthanizing the mice dramatically reduced externalization of PS by WT T reg cells (Fig. 3 C). This treatment also efficiently protected T reg cells in the highly NICD-susceptible $CD38^{-/-}$ background (Fig. 3 C). Consistently, T reg cells from both WT and $CD38^{-/-}$ mice treated with s+16a shed neither CD62L nor CD27, another surface molecule sensitive to P2X7 activation (Moon et al., 2006), when returned to 37°C (Fig. 3 C).

NAD^+ influences the suppressive activity of T reg cells in vitro

It has been observed that T reg cells with a $CD62L^{lo}$ phenotype display low suppressive functions (Fu et al., 2004; Ermann et al., 2005). Considering that this phenotype may result from P2X7 activation, we evaluated the consequences of NAD^+ on T reg cell function in a classical in vitro suppression assay. $CD4^+CD25^+$ T reg cells from WT or $ART2^{-/-}$ mice were added to $CD4^+CD25^-$ T cells from $ART2^{-/-}$ mice and

activated with Con A in the presence of increasing NAD^+ concentrations. Even in the absence of exogenously added NAD^+, T reg cells from $ART2^{-/-}$ mice were more efficient at suppressing T cell proliferation than their WT counterparts (Fig. 4 A), which is consistent with their resistance to NAD^+ released during cell preparation (Fig. 3). Addition of exogenous NAD^+ further reduced the suppressive effect of WT T reg cells in a dose-dependent manner, whereas it had no effect on the function of T reg cells from $ART2^{-/-}$ mice (Fig. 4 A). Consistently, $ART2^{-/-}$ T reg cells were more efficient than WT T reg cells at suppressing T cell proliferation over a broad range of T reg/T conv cell ratios in the absence of any exogenous NAD^+ addition (Fig. 4 B). These results may help explain why classical in vitro suppression assays require much higher T reg/T conv cell ratios than are observed in vivo. The weak suppressive capacities of T reg cells assayed in vitro may be, in part, a consequence of exposure to NAD^+ during cell preparation. Indeed, when T reg cells are insensitive to NAD^+, a T reg/T conv cell ratio of 1:10 is sufficient to suppress the proliferative response by 50%, whereas a number of T reg cells that is five times higher is required for obtaining the same effect with WT T reg cells.

Manipulating the ART2–P2X7 pathway to modulate the antitumor response

The higher sensitivity of T reg cells to NAD^+ may offer an opportunity to selectively manipulate the T reg cell compartment in vivo by acting on the ART2–P2X7 pathway. To explore this possibility, we used the EL4 tumor model, in which the antitumor response is naturally suppressed by T reg cells and in which T reg cell depletion is sufficient to elicit an effective immune response and to inhibit tumor growth (Onizuka et al., 1999). As expected, T reg cell depletion by administration of an anti-CD25 antibody before transfer of tumor cells effectively blocked tumor progression. Remarkably, a single i.v. injection of 10 mg NAD^+ in $CD38^{-/-}$ mice or of 60 mg NAD^+ in WT mice, i.e., doses that effectively deplete 75–80% T reg cells (Fig. 1), 1 d before transfer of EL4 cells led to efficient control of tumor growth (Fig. 5 A). It is of note that the EL4 cell expresses neither ART2.2 nor CD25 and is insensitive to NAD^+ (Fig. S1). Remarkably, the antitumor effect of NAD^+ was fully reverted when mice were pretreated with an Fc fusion protein of the ART2.2-blocking s+16a sdAb, which is consistent with the notion that T reg cells are protected from NICD by this ART2.2-blocking Ab (Fig. 5 A). Similar effects of NAD^+ on tumor growth were observed with other lymphoid and nonlymphoid tumors, i.e., the EG7 lymphoma (Fig. 5 B), the MCA fibrosarcoma (Fig. S2), and the B16 melanoma (Fig. 6 A).

Mice were further analyzed for antitumor T cell responses. NAD-treated mice that had rejected EG7 tumor were completely resistant to a secondary tumor challenge 2 mo later (Fig. 5 C), suggesting that a specific and efficient memory T cell antitumor response had been generated in those mice. Analysis of blood samples 12–14 d after primary tumor inoculation demonstrated that NAD-treated

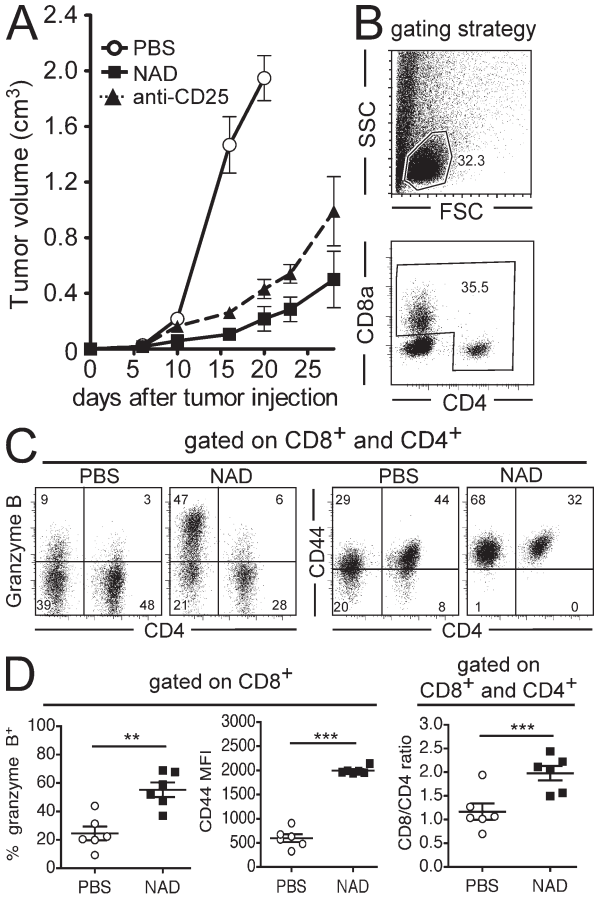

Figure 6. Effect of in vivo administration of NAD^+ on the immune response against B16-Ova tumors. Groups of mice ($n = 6$) received systemic injections of PBS on day −1 (control), anti-CD25 (PC-61) antibody on day −4 and −1, or 60 mg NAD^+ on day −1, followed by the inoculation of 2×10^5 B16-Ova tumor cells on day 0. (A) Tumor growth was followed over time. (B–D) Groups of mice ($n = 6$–7) treated as in A were killed at days 12–14 for flow cytometry analysis of TILs. (B) Gating strategy of $CD4^+$ and $CD8^+$ TILs. (C and D) Representative FACS profiles (C) and quantitative analyses (D) of cell surface CD44, intracellular GzB, and the ratios of $CD8^+/CD4^+$ TILs. Data are representative of three independent experiments. Statistical Mann-Whitney *U* tests showed significant differences between tumor volumes in all experiments when comparing PBS- to NAD-treated animals after day 12. Horizontal lines show the mean. **, $P < 0.01$; ***, $P < 0.001$. Error bars represent SEM.

mice displayed significantly higher frequencies of $CD4^+$ and $CD8^+$ cells expressing the CD44 activation marker, of $CD8^+$ cells expressing granzyme B (GzB), and of anti–Ova-specific $CD8^+$ cells (Fig. 5 D). Finally, the phenotype of tumor-infiltrating lymphocytes (TILs) was analyzed. As the lymphoid EL4 and EG7 tumors express CD4, we turned to the B16-Ova model to better discriminate TILs from tumor cells. $CD4^+Foxp3^+$ cells could be detected among TILs at similar frequencies to the control group, which is consistent with a recovery of the T reg cell compartment 14 d after NAD^+ injection (unpublished data). However, TILs from NAD-treated mice displayed significantly higher frequencies of $CD8^+GzB^+$ cells with higher cell surface levels of the activation

marker CD44 compared with TILs from PBS-treated mice (Fig. 6, C and D). Collectively, these results provide proof of principle that T reg cells can be depleted in mice by a single injection of NAD^+ to promote an antitumor response and open new perspectives to pharmacologically manipulate the T reg cell compartment by molecules acting on the ART2–P2X7 pathway.

MATERIALS AND METHODS

Mice. C57BL/6 (B6) mice were obtained from Centre d'Elevage Janvier or from The Jackson Laboratory. $CD38^{-/-}$, $P2X7^{-/-}$, and $ART2^{-/-}$ mice were backcrossed onto the B6 background for 12 generations as described previously (Cockayne et al., 1998; Solle et al., 2001; Seman et al., 2003; Krebs et al., 2005; Scheuplein et al., 2009). DEREG (B6) mice expressing DTR-eGFP under the control of the *foxp3* promoter (Lahl et al., 2007) were backcrossed onto $ART2^{-/-}$, $CD38^{-/-}$, or $P2X7^{-/-}$ backgrounds. All animal experiments were approved by the local institutional ethic committee (Comité régional d'éthique en expérimentation animale de Normandie).

Reagents, antibodies, and flow cytometry. NAD^+ and Con A were obtained from Sigma-Aldrich. Fluorescently labeled α-CD4 (L3T4), α-CD25 (PC61), α-CD27 (LG.3A10), α-CD62L (MEL-14), and α-CD103 (M290) mAb, unlabeled α-CD16/CD32 antibodies, and annexin V were all obtained from BD. Fluorescently labeled α-CD44 (IM7) and α-Foxp3 (FJK-16s) antibodies were purchased from eBioscience and α-GzB (clone GB12) from Invitrogen. Intracellular Foxp3 and GzB staining was performed according to the manufacturer's protocol. PE-conjugated H-$2K^b$/$Ova_{257-264}$ pentamers were used to detect $CD8^+$ cells specifically recognizing the immunodominant SIINFEKL ovalbumin peptide using the manufacturer's protocol (ProImmune). α-ProimmuneART2.2 (Nika102), α-ProimmuneP2X7 (Hano44 or K1G), and the ART2.2-inhibiting s+16a recombinant sdAb were previously described (Koch-Nolte et al., 1999, 2007; Adriouch et al., 2005). The bivalent s+16a-Fc antibody was obtained by genetic fusion of s+16a to the mouse IgG1 Fc domains (Scheuplein et al., 2010). Where indicated, 5 µg of purified s+16a-Fc antibody or 300 µg s+16a were injected i.v. to block ART2.2 activity in vivo. Flow cytometry measurements of single-cell suspensions were performed using standard procedures on a FACSCalibur or a FACSCanto (BD) and analyses were made using FlowJo software (Tree Star, Inc.).

NAD treatment in vivo. $CD38^{-/-}$ and WT mice were treated i.v. with 10 or 60 mg NAD in 100–200 µl PBS solution adjusted to pH 7.4. 24 h later, single-cell suspensions prepared from LN, spleen, and blood were analyzed by flow cytometry. Absolute T cell numbers were enumerated from six pooled LNs (inguinal, axillary, and brachial).

Assays for PS exposure and for shedding of CD27 and CD62L. These assays were previously described (Seman et al., 2003; Moon et al., 2006; Adriouch et al., 2007; Scheuplein et al., 2009). In brief, lymphocytes were harvested in cold D-PBS supplemented with 5% FCS, washed, and further incubated for 15 min either at 4 or 37°C in complete RPMI medium. Cells were then washed and stained with fluorescently conjugated α-CD62L, α-CD27, and other indicated mAbs. For PS exposure assays, cells were labeled with indicated antibodies, washed, and incubated in annexin V binding buffer for 20 min on ice with 1 µg/ml APC-conjugated annexin V and 10 µg/m lPI according to the recommendation of the supplier (BD).

Functional T reg cell assays in vitro. Total $CD4^+$ lymphocytes were purified from pooled LNs of indicated mice using the CD4 negative isolation kit (Invitrogen). Cells were further sorted using α–CD25-PE and anti-PE magnetic beads (Miltenyi Biotec). The purities of T conv and T reg cells obtained after isolation were always >95%. T reg cells were added at different ratios to T conv responder cells (5×10^4/well) isolated either from WT or $ART2.2^{-/-}$ mice as indicated in the figure legends. Cells were then activated for 72 h by 2.5 µg/ml Con A in the presence of 5×10^4 splenocytes from syngeneic $CD3^{-/-}$ mice and pulsed with 0.5 µCi/well of [^{3}H]-TdR for the last 24 h of culture. Where indicated, NAD^+ was also added at the beginning of the co-culture.

Tumor models. All of the following tumor cells used were from the B6 background: EL4, EL4-Ova (EG7), MCA101-Ova (Zeelenberg et al., 2008), and B16-Ova. $CD38^{-/-}$ or WT mice received, respectively, 10 or 60 mg NAD^+ i.v. at day −1. Control groups were treated in parallel with PBS, 5 µg ART2-blocking s+16a-Fc llama sdAb at day −2, and 250 µg α-CD25 mAb PC-61 at days −4 and −1. All mice were then injected subcutaneously on day 0 with 2×10^5 tumor cells into their shaved backs and tumor sizes were measured with a digital caliper three times a week. Tumor volume was calculated as length × width × [(length + width)/2]. Analysis of TILs was performed at days 12–14 by digestion of sliced tumor tissue with collagenase/dispase/DNase solution for 30 min at 37°C followed by filtration and centrifugation on a 40–70% Percoll density gradient.

Statistical analysis. All data are shown as mean values and error bars represent SEM. For statistical comparisons, the Mann-Whitney *U* test was used. Differences were considered to be statistically significant when p-values were <0.05. All calculations were performed using Prism software (GraphPad Software, Inc.).

Online supplemental material. Fig. S1 shows that EL4, EG7, and MCA-Ova tumor cells are insensitive to NAD^+-induced cell death in vitro. Fig. S2 shows the effect of in vivo administration of NAD^+ on MCA-Ova tumor growth. Online supplemental material is available at http://www.jem.org/cgi/content/full/jem.20091154/DC1.

We acknowledge Frances Lund (University of Rochester) and Christopher Gabel (Pfizer Corporation) for providing $CD38^{-/-}$ and $P2X7^{-/-}$, respectively, and Clotilde Théry for providing the MCA-Ova tumor model. We thank Laurent Drouot, Christophe Arnoult, and Laetitia Jean (Rouen) and Marion Nissen, Valea Schumacher, and Fabienne Seyfried (Hamburg) for their technical help during the study. We thank Hans-Willi Mittrücker (Hamburg) for critical reading of the manuscript.

The study was funded partly by Association pour la Recherche sur le Cancer, Association Française contre les Myopathies, and Deutsche Forschungsgemeinschaft.

F. Haag and F. Koch-Nolte disclose that they receive an honorarium from Analytical Services GmbH, a 100% subsidiary of the University Medical Center Hamburg-Eppendorf, for sales of antibodies developed in their laboratory, including the anti-ART2.2 and anti-P2X7 antibodies described in this manuscript. The authors have no additional financial interests.

Submitted: 27 May 2009
Accepted: 22 September 2010

REFERENCES

Adriouch, S., G. Dubberke, P. Diessenbacher, F. Rassendren, M. Seman, F. Haag, and F. Koch-Nolte. 2005. Probing the expression and function of the P2X7 purinoceptor with antibodies raised by genetic immunization. *Cell. Immunol.* 236:72–77. doi:10.1016/j.cellimm.2005.08.011

Adriouch, S., S. Hubert, S. Pechberty, F. Koch-Nolte, F. Haag, and M. Seman. 2007. NAD+ released during inflammation participates in T cell homeostasis by inducing ART2-mediated death of naive T cells in vivo. *J. Immunol.* 179:186–194.

Adriouch, S., P. Bannas, N. Schwarz, R. Fliegert, A.H. Guse, M. Seman, F. Haag, and F. Koch-Nolte. 2008. ADP-ribosylation at R125 gates the P2X7 ion channel by presenting a covalent ligand to its nucleotide binding site. *FASEB J.* 22:861–869. doi:10.1096/fj.07-9294com

Aswad, F., H. Kawamura, and G. Dennert. 2005. High sensitivity of CD4+CD25+ regulatory T cells to extracellular metabolites nicotinamide adenine dinucleotide and ATP: a role for P2X7 receptors. *J. Immunol.* 175:3075–3083.

Bruzzone, S., L. Franco, L. Guida, E. Zocchi, P. Contini, A. Bisso, C. Usai, and A. De Flora. 2001. A self-restricted CD38-connexin 43 cross-talk affects NAD+ and cyclic ADP-ribose metabolism and regulates intracellular calcium in 3T3 fibroblasts. *J. Biol. Chem.* 276:48300–48308.

Cockayne, D.A., T. Muchamuel, J.C. Grimaldi, H. Muller-Steffner, T.D. Randall, F.E. Lund, R. Murray, F. Schuber, and M.C. Howard. 1998. Mice deficient for the ecto-nicotinamide adenine dinucleotide glycohydrolase CD38 exhibit altered humoral immune responses. *Blood.* 92:1324–1333.

Contreras, J.E., H.A. Sánchez, E.A. Eugenin, D. Speidel, M. Theis, K. Willecke, F.F. Bukauskas, M.V. Bennett, and J.C. Sáez. 2002. Metabolic inhibition induces opening of unapposed connexin 43 gap junction hemichannels and reduces gap junctional communication in cortical astrocytes in culture. *Proc. Natl. Acad. Sci. USA.* 99:495–500. doi:10.1073/pnas.012589799

Cortez-Retamozo, V., N. Backmann, P.D. Senter, U. Wernery, P. De Baetselier, S. Muyldermans, and H. Revets. 2004. Efficient cancer therapy with a nanobody-based conjugate. *Cancer Res.* 64:2853–2857. doi:10.1158/0008-5472.CAN-03-3935

De Genst, E., K. Silence, K. Decanniere, K. Conrath, R. Loris, J. Kinne, S. Muyldermans, and L. Wyns. 2006. Molecular basis for the preferential cleft recognition by dromedary heavy-chain antibodies. *Proc. Natl. Acad. Sci. USA.* 103:4586–4591. doi:10.1073/pnas.0505379103

Di Virgilio, F. 2007. Liaisons dangereuses: P2X(7) and the inflammasome. *Trends Pharmacol. Sci.* 28:465–472. doi:10.1016/j.tips.2007.07.002

Di Virgilio, F., P. Chiozzi, D. Ferrari, S. Falzoni, J.M. Sanz, A. Morelli, M. Torboli, G. Bolognesi, and O.R. Baricordi. 2001. Nucleotide receptors: an emerging family of regulatory molecules in blood cells. *Blood.* 97:587–600. doi:10.1182/blood.V97.3.587

Ermann, J., P. Hoffmann, M. Edinger, S. Dutt, F.G. Blankenberg, J.P. Higgins, R.S. Negrin, C.G. Fathman, and S. Strober. 2005. Only the CD62L+ subpopulation of CD4+CD25+ regulatory T cells protects from lethal acute GVHD. *Blood.* 105:2220–2226. doi:10.1182/blood-2004-05-2044

Fontenot, J.D., M.A. Gavin, and A.Y. Rudensky. 2003. Foxp3 programs the development and function of CD4+CD25+ regulatory T cells. *Nat. Immunol.* 4:330–336. doi:10.1038/ni904

Fu, S., A.C. Yopp, X. Mao, D. Chen, N. Zhang, D. Chen, M. Mao, Y. Ding, and J.S. Bromberg. 2004. CD4+ CD25+ CD62+ T-regulatory cell subset has optimal suppressive and proliferative potential. *Am. J. Transplant.* 4:65–78. doi:10.1046/j.1600-6143.2003.00293.x

Hori, S., T. Nomura, and S. Sakaguchi. 2003. Control of regulatory T cell development by the transcription factor Foxp3. *Science.* 299:1057–1061. doi:10.1126/science.1079490

Khattri, R., D. Kasprowicz, T. Cox, M. Mortrud, M.W. Appleby, M.E. Brunkow, S.F. Ziegler, and F. Ramsdell. 2001. The amount of scurfin protein determines peripheral T cell number and responsiveness. *J. Immunol.* 167:6312–6320.

Koch-Nolte, F., T. Duffy, M. Nissen, S. Kahl, N. Killeen, V. Ablamunits, F. Haag, and E.H. Leiter. 1999. A new monoclonal antibody detects a developmentally regulated mouse ecto-ADP-ribosyltransferase on T cells: subset distribution, inbred strain variation, and modulation upon T cell activation. *J. Immunol.* 163:6014–6022.

Koch-Nolte, F., J. Reyelt, B. Schössow, N. Schwarz, F. Scheuplein, S. Rothenburg, F. Haag, V. Alzogaray, A. Cauerhff, and F.A. Goldbaum. 2007. Single domain antibodies from llama effectively and specifically block T cell ecto-ADP-ribosyltransferase ART2.2 in vivo. *FASEB J.* 21:3490–3498. doi:10.1096/fj.07-8661com

Krebs, C., S. Adriouch, F. Braasch, W. Koestner, E.H. Leiter, M. Seman, F.E. Lund, N. Oppenheimer, F. Haag, and F. Koch-Nolte. 2005. CD38 controls ADP-ribosyltransferase-2-catalyzed ADP-ribosylation of T cell surface proteins. *J. Immunol.* 174:3298–3305.

Lahl, K., C. Loddenkemper, C. Drouin, J. Freyer, J. Arnason, G. Eberl, A. Hamann, H. Wagner, J. Huehn, and T. Sparwasser. 2007. Selective depletion of Foxp3$^+$ regulatory T cells induces a scurfy-like disease. *J. Exp. Med.* 204:57–63. doi:10.1084/jem.20061852

Moon, H., H.Y. Na, K.H. Chong, and T.J. Kim. 2006. P2X7 receptor-dependent ATP-induced shedding of CD27 in mouse lymphocytes. *Immunol. Lett.* 102:98–105. doi:10.1016/j.imlet.2005.08.004

Ochs, H.D., S.F. Ziegler, and T.R. Torgerson. 2005. FOXP3 acts as a rheostat of the immune response. *Immunol. Rev.* 203:156–164. doi:10.1111/j.0105-2896.2005.00231.x

Onizuka, S., I. Tawara, J. Shimizu, S. Sakaguchi, T. Fujita, and E. Nakayama. 1999. Tumor rejection by in vivo administration of anti-CD25 (interleukin-2 receptor alpha) monoclonal antibody. *Cancer Res.* 59:3128–3133.

Partida-Sánchez, S., D.A. Cockayne, S. Monard, E.L. Jacobson, N. Oppenheimer, B. Garvy, K. Kusser, S. Goodrich, M. Howard, A. Harmsen, et al. 2001. Cyclic ADP-ribose production by CD38 regulates intracellular calcium release, extracellular calcium influx and chemotaxis in neutrophils and is required for bacterial clearance in vivo. *Nat. Med.* 7:1209–1216. doi:10.1038/nm1101-1209

Sakaguchi, S. 2005. Naturally arising Foxp3-expressing CD25+CD4+ regulatory T cells in immunological tolerance to self and non-self. *Nat. Immunol.* 6:345–352. doi:10.1038/ni1178

Scheuplein, F., N. Schwarz, S. Adriouch, C. Krebs, P. Bannas, B. Rissiek, M. Seman, F. Haag, and F. Koch-Nolte. 2009. NAD+ and ATP released from injured cells induce P2X7-dependent shedding of CD62L and externalization of phosphatidylserine by murine T cells. *J. Immunol.* 182:2898–2908. doi:10.4049/jimmunol.0801711

Scheuplein, F., B. Rissiek, J.P. Driver, Y.G. Chen, F. Koch-Nolte, and D.V. Serreze. 2010. A recombinant heavy chain antibody approach blocks ART2 mediated deletion of an iNKT cell population that upon activation inhibits autoimmune diabetes. *J. Autoimmun.* 34:145–154. doi:10.1016/j.jaut.2009.08.012

Seman, M., S. Adriouch, F. Scheuplein, C. Krebs, D. Freese, G. Glowacki, P. Deterre, F. Haag, and F. Koch-Nolte. 2003. NAD-induced T cell death: ADP-ribosylation of cell surface proteins by ART2 activates the cytolytic P2X7 purinoceptor. *Immunity.* 19:571–582. doi:10.1016/S1074-7613(03)00266-8

Solle, M., J. Labasi, D.G. Perregaux, E. Stam, N. Petrushova, B.H. Koller, R.J. Griffiths, and C.A. Gabel. 2001. Altered cytokine production in mice lacking P2X(7) receptors. *J. Biol. Chem.* 276:125–132. doi:10.1074/jbc.M006781200

Zeelenberg, I.S., M. Ostrowski, S. Krumeich, A. Bobrie, C. Jancic, A. Boissonnas, A. Delcayre, J.B. Le Pecq, B. Combadière, S. Amigorena, and C. Théry. 2008. Targeting tumor antigens to secreted membrane vesicles in vivo induces efficient antitumor immune responses. *Cancer Res.* 68:1228–1235. doi:10.1158/0008-5472.CAN-07-3163